PERGAMON

International Journal of Heat and Mass Transfer 45 (2002) 2129–2139

International Journal of HEAT and MASS TRANSFER

www.elsevier.com/locate/ijhmt

On the application of the exponential wide band model to the calculation of radiative heat transfer in one- and two-dimensional enclosures

Jochen Ströhle [a,*], Pedro J. Coelho [b]

[a] *Institute of Process Engineering and Power Plant Technology, University of Stuttgart, Pfaffenwaldring 23, Stuttgart D-70550, Germany*
[b] *Instituto Superior Técnico, Technical University of Lisbon, Av. Rovisco Pais, Lisboa 1049-001, Portugal*

Received 19 April 2001; received in revised form 25 July 2001

Abstract

Various implementations of the exponential wide band model (EWBM) are used to model radiative heat transfer in one- and two-dimensional enclosures containing CO_2 and H_2O. These are, first, the original banded approach using the four-region approximation for the total band absorption, second, a numerical integration of the spectral transmittance, and third, the wide band correlated *k*-distribution method (CKM). A correlated and a non-correlated formulation are used to solve the radiative transfer equation. In two-dimensional enclosures, these formulations are implemented using a ray tracing method (RTM) and the discrete ordinates method (DOM), respectively. The wide band CKM is found to be the best choice concerning accuracy and computational effort. © 2002 Elsevier Science Ltd. All rights reserved.

Keywords: Heat transfer; Modeling; Radiation

1. Introduction

The numerical simulation of radiative heat transfer in combustion systems is very complex since the radiative properties of the combustion gases are strongly correlated with the wave number of the radiative intensity. Several models exist to account for the dependency of the absorptance of combustion gases on the wave number spectrum. Line-by-line (LBL) models [1] calculate the radiative properties for each individual line. They yield very accurate results, but are computationally far too expensive for engineering applications, since the whole spectrum consists of millions of single lines. Narrow band models [2] divide the spectrum in a specified number of narrow bands within which the properties are calculated. But due to the large number of bands, these models are still not efficient for multi-dimensional computations.

In order to further simplify the calculations, wide band models treat each rotational–vibrational band as a whole. Edwards and Balakrishnan [3] developed the exponential wide band model (EWBM) assuming an exponential function of the line intensity around a band centre. The total band absorption is approximated by a four-region expression and the band transmittance is calculated using a grey band assumption. Several researchers have worked on this model. Modak [4] found improved parameters for the pure rotational band of water vapour. Docherty and Fairweather [5] successfully applied the EWBM to flame calculations using the discrete transfer method. Since the grey band assumption leads to large errors for small path lengths, Komornicki and Tomeczek [6] modified the EWBM by tabulating the absorptance of the main bands in terms of temperature and optical depth. Cumber et al. [7] reached improved results by dividing the entire wave number spectrum into a fixed number of intervals and calculating the transmittance of each interval directly from the spectral transmittance.

One of the major problems of the EWBM is that it computes transmittances dependent on path length instead of absorption coefficients, which are required for the solution of the radiative transfer equation (RTE).

* Corresponding author. Fax: +49-711-685-3491.
E-mail address: stroehle@ivd.uni-stuttgart.de (J. Ströhle).

0017-9310/02/$ - see front matter © 2002 Elsevier Science Ltd. All rights reserved.
PII: S0017-9310(01)00311-8

Nomenclature

A	band absorption (cm^{-1})
a_j	weight of grey gas
$C_{i,j}$	coefficient in Eq. (15)
E_n	exponential integral function
F	blackbody fractional function
I	radiative intensity ($W\ m^{-2}\ sr^{-1}$)
$\vec{n}$	normal vector
p_i	pole
q	heat flux density ($W\ m^{-2}$)
S/d	line intensity to line spacing ratio ($m^2 g^{-1}$)
s	path along a ray (m)
T	temperature (K)
w	quadrature weight
X	absorber density-path length product ($g\ m^{-2}$)

Greek symbols

α	integrated band intensity ($cm^{-1}\ (g^{-1}\ m^2)$)
β	line width-to-spacing parameter
Δv	band width (cm^{-1})
ε	emissivity
η	x-direction cosine
κ	absorption coefficient (m^{-1})
v	wave number (cm^{-1})
ξ	reordered wave number (cm^{-1})
ρ	gas density ($g\ m^{-3}$)
τ	transmittance
τ_H	optical depth at band head
Ω	solid angle (sr)
ω	band width parameter (cm^{-1})

Subscripts

b	blackbody
c	centre limit
j	grey gas
k	band
l	lower limit
n	computational cell face
u	upper limit
w	wall
v	spectral

Superscript

m	direction
$*$	dimensionless variables

This greatly complicates the coupling between the EWBM and the RTE. Recently, the k-distribution method, formerly developed for atmospheric radiation [8,9], has received increased attention in the heat transfer community [10]. In this method, the wave number spectrum is reordered to yield a smooth function of the absorption coefficient, so that a set of mean values of the absorption coefficient can be introduced for a certain wave number interval. If narrow band intervals are considered, the method becomes computational too expensive for most engineering applications. However, wide band intervals may also be used yielding the wide band correlated k-distribution method (CKM). Lee et al. [11] and Parthasarathy et al. [12] developed reordered wave number distribution functions of the absorption coefficient based on continuous correlations for the wide band absorption. Marin and Buckius [13,14] found simple correlations to calculate the absorption coefficient directly from the cumulative distribution function. Denison and Fiveland [15] presented a correlation in closed form for the reordered wave number that closely approximates the four-region expression for the wide band absorption.

The discrete ordinates method (DOM) [16,17] is one of the most popular radiation models presently available because it combines accuracy, flexibility and computational economy. However, like other differential radiation solvers, the DOM is difficult to couple with the EWBM. The exact implementation has been presented in [18] for black walls, and later extended to diffusely reflecting walls for the case of one-dimensional problems [19]. This rigorous treatment is generally referred to as the correlated formulation. The extension of this formulation to multi-dimensional problems is not feasible. Therefore, the correlated formulation has to be used along with a ray tracing method (RTM) rather than the DOM. The non-correlated formulation allows a straightforward application of the EWBM to the solution of the RTE using the DOM for both one- and multi-dimensional problems, but it is often unsatisfactory [20]. The wide band CKM is also easily coupled with the DOM.

The aim of this study is to compare the different approaches of the EWBM and to find an optimal solution for engineering calculations for multi-dimensional cases considering both numerical accuracy and efficiency. Five different approaches are considered, namely the four-region expression of the EWBM applied to the correlated and non-correlated formulations, the integration of the spectral transmittance given by the EWBM also applied to the correlated and non-correlated formulations, and the wide band CKM applied to the DOM.

The implementation of three of these five approaches present some original features. Hence, the four-region expression of the EWBM is applied to the non-correlated formulation using fixed band limits. It has been shown [21] that this strategy yields more accurate results than the original approach. Cumber et al. [7] have only used the non-correlated formulation for their integration

method, whereas both the correlated and non-correlated formulations are applied to this method in the present study. Finally, the correlations of Denison and Fiveland [15] used in the wide band CKM, that had previously only been used to solve one-dimensional homogeneous radiative transfer problems, are applied here to multi-dimensional non-homogeneous media.

The correlated and non-correlated formulations are briefly described in the next section. Then, the different implementations of the EWBM are outlined. A comparison between predicted and measured emissivity spectra is given in Section 4. The radiative transfer in one- and two-dimensional enclosures is presented and discussed in Section 5, and the paper ends with a summary of the main conclusions.

2. Radiative transfer equation

The change of spectral intensity I_ν along a path s is described by the RTE. Using a band model, the intensity is averaged over the width of the band, indicated by overbar symbols. The wave number averaged form of the RTE in an absorbing and emitting, non-scattering medium can be written as

$$\frac{\mathrm{d}}{\mathrm{d}s}\bar{I}_\nu = \bar{\kappa}_\nu \bar{I}_{\mathrm{b},\nu} - \overline{\kappa_\nu I_\nu}. \tag{1}$$

Scattering can be neglected in gaseous media without large particles, as that appearing in natural gas flames. While the Planck function $I_{\mathrm{b},\nu}$ is smooth over the wave number spectrum, the intensity I_ν is strongly correlated with the absorption coefficient κ. Using an exact formulation (see [18]), the correlated intensity along a path s is expressed in terms of transmittance as needed for the EWBM

$$\bar{I}_\nu = \bar{I}_{\nu,\mathrm{w}}\bar{\tau}_\nu(s_\mathrm{w} \to s) + \int_{s_\mathrm{w}}^{s} \frac{\partial}{\partial s'}\bar{\tau}_\nu(s' \to s)\bar{I}_{\mathrm{b},\nu}\,\mathrm{d}s'. \tag{2}$$

The intensity $I_{\nu,\mathrm{w}}$ originating from the point s_w on a wall is the blackbody intensity of the wall $I_{\mathrm{b},\nu,\mathrm{w}}$ in the case of a black wall. For grey, diffusely reflecting walls, an analytical formulation of the spectral averaged intensity is not possible (see [19]). Thus, a zeroth-degree closure is introduced assuming the intensity onto the wall to be independent of wave number within a band

$$\bar{I}_{\nu,0} = \varepsilon_\mathrm{w}\bar{I}_{\mathrm{b},\nu,\mathrm{w}} + \frac{1-\varepsilon_\mathrm{w}}{\pi}\int_{\vec{s}\cdot\vec{n}_\mathrm{w}<0} \bar{I}_\nu\left|\vec{s}\cdot\vec{n}_\mathrm{w}\right|\mathrm{d}\Omega. \tag{3}$$

In this equation, ε_w is the wall emissivity, $\vec{s}$ is the direction of propagation of the radiative intensity, $\vec{n}_\mathrm{w}$ is the unit normal vector at the wall and Ω is the solid angle. The zeroth-degree closure is exact for non-reflecting (i.e., black) walls. The accuracy of this closure assumption is expected to decrease as the reflectivity of the walls increases. However, even in the case of highly reflecting walls, the zeroth-degree closure may be a good approximation provided that the medium is optically thick, because in this case radiation leaving the walls will be rapidly absorbed by the medium.

When the intensity along a line of sight is discretized into homogeneous cells, the intensity at point n depends on all upstream blackbody intensities and on all transmittances $\tau_{i\to n}$ from each upstream cell i to n. Following the notation in Fig. 1, the spatial discretized form of Eq. (2) is

$$\bar{I}_{\nu,n} = \bar{I}_{\nu,0}\bar{\tau}_{\nu,0\to n} + \sum_{i=0}^{n-1}\left(\bar{\tau}_{\nu,i+1\to n} - \bar{\tau}_{\nu,i\to n}\right)\bar{I}_{\mathrm{b},\nu,i+1/2}. \tag{4}$$

The Curtis–Godson approximation [22] is applied to calculate transmittances for a non-isothermal or non-homogeneous medium. The calculation of the difference of transmittance in Eq. (4) is not straightforward when the band limits are not constant, i.e. when the four-region expression is used. In this study, the band limits are pre-defined using the limits for the calculation of $\bar{\tau}_{\nu,0\to n}$. A pre-defined band with the lower limit $\nu_{\mathrm{fix},l}$, and upper limit $\nu_{\mathrm{fix},u}$, is split into sub-bands using the lower limits $\nu_{1,l}$, $\nu_{2,l}$ and upper limits $\nu_{1,u}$, $\nu_{2,u}$ for two consecutive transmittances $\tau_1 = \bar{\tau}_{\nu,i\to n}$ and $\tau_2 = \bar{\tau}_{\nu,i+1\to n}$, as illustrated in Fig. 2. In each sub-band, the transmittance difference

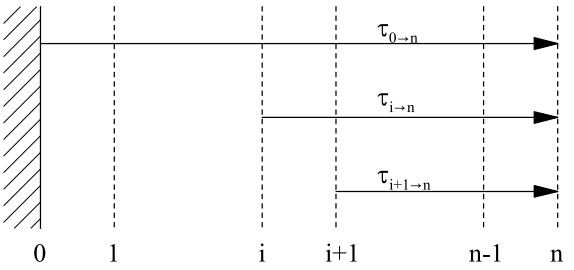

Fig. 1. Spatial discretization along a line of sight.

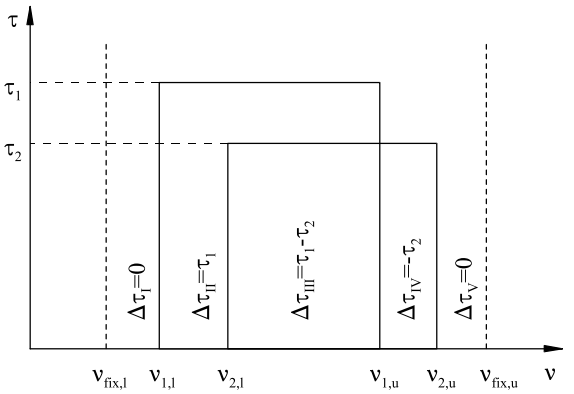

Fig. 2. Calculation of transmittance difference.

is computed individually, and the transmitted blackbody intensities are summed afterwards.

The correlated formulation described above may lead to excessive computer times. Therefore, several authors [5,7,18] have used an alternative formulation that neglects the correlation between the radiation intensity and the absorption coefficient, and leads to the far simpler recurrence relation

$$\bar{I}_{v,n} = \bar{I}_{v,n-1}\bar{\tau}_{v,n-1\to n} + \bar{I}_{\mathrm{b},v,n-1/2}\left(1-\bar{\tau}_{v,n-1\to n}\right). \tag{5}$$

Although physically unrealistic, this formulation has often been used, and may lead to acceptable results [5,7], but general conditions required to obtain accurate results have not been established.

The intensity distribution in a one-dimensional enclosure is calculated from Eqs. (4) or (5) using a discrete ordinates quadrature for angular discretization. The transmittance of a gas layer with thickness Δx is computed based on the path length $L = \Delta x/\eta^m$ where η^m is the x direction cosine of direction m. The wall heat flux density q_w is derived from the sum of all incoming intensities of all bands k and directions m with their quadrature weights w^m

$$q_\mathrm{w} = \sum_k \sum_{\substack{m \\ \vec{s}^m\cdot\vec{n}_\mathrm{w}<0}} I_k^m w^m |\eta^m|. \tag{6}$$

Application of Eq. (4) to multi-dimensional enclosures is very time consuming since an RTM has to be applied. The intensity is traced from each cell face to the wall for all directions. If a differential solver of the RTE is employed, such as the DOM, the absorption coefficient of the medium must be known. This is accomplished by assuming that the medium is grey within a wide band, and using Beer's law to calculate the absorption coefficient from the mean transmissivity within a band. However, the absorption coefficient is a local property, independent of any path length, while the mean transmissivity requires the specification of the path length. There are two possible choices for the mean transmissivity used to compute the local absorption coefficient at a given point within the medium and for a given wide band: the mean beam length of the local cell, or the mean beam length of the whole domain. One reason to select the second approach is that in the case of a homogeneous and isothermal medium, the radiation intensity at the end of a line of sight is independent of the grid size if the mean beam length of the whole domain is used. In the present work, both methods have been tried, but only the second one, which has given better results is selected.

When the wide band CKM is used, the reordered wave number spectrum is discretized into a set of grey gases with absorption coefficients κ_j. The RTE is solved for all grey gases

$$\frac{\mathrm{d}}{\mathrm{d}s} I_j = \kappa_j (a_j I_b - I_j). \tag{7}$$

where a_j are the weights to be defined in the following section. The DOM may be used to solve this equation for all grey gases.

3. Exponential wide band model

Only a short overview of the EWBM is given here since a detailed description may be found in [22]. The model is based on the fact that absorption and emission of infra-red radiation from gases is generally concentrated within several bands resulting from changes of energy storage of the molecules between vibrational modes. Energy changes between rotational modes lead to a large number of spectral lines within each band. A detailed knowledge of the position, shape and intensity of theses lines is considered to be unimportant in the EWBM, instead the line intensity is approximated by an exponentially decreasing function. The radiative properties are obtained by specifying three model parameters that characterize a given absorption band, which are an integrated band intensity α, a mean line width-to-spacing parameter β, and a band width parameter ω. These parameters are in general a function of temperature evaluated by Edwards and Balakrishnan [3]. The mean line intensity to spectral line spacing ratio S/d is given by one of three simple exponential functions depending on whether a lower limit v_l, upper limit v_u or band centre wave number v_c is used to prescribe the position of the band head

$$S/d = (\alpha/\omega)\mathrm{e}^{-(v_\mathrm{u}-v)/\omega} \quad \text{(upper limit)}, \tag{8a}$$

$$S/d = (\alpha/\omega)\mathrm{e}^{-(v-v_\mathrm{l})/\omega} \quad \text{(lower limit)}, \tag{8b}$$

$$S/d = (\alpha/\omega)\mathrm{e}^{-2|v_\mathrm{c}-v|/\omega} \quad \text{(band centre)}. \tag{8c}$$

The spectral transmittance of the band at wave number v is derived from

$$\tau_v = \exp\left[\frac{-(S/d)X}{(1+(S/d)X/\beta)^{1/2}}\right]. \tag{9}$$

3.1. Four-region method

Various methods are possible to calculate the transmittance of an entire band. The original method of Edwards [22] approximates the band absorption A using the so-called four-region expression

$$A^* = \tau_\mathrm{H} \quad \text{for } \tau_\mathrm{H} \leqslant 1,\ \ \tau_\mathrm{H} \leqslant \beta, \tag{10a}$$

$$A^* = (4\beta\tau_\mathrm{H})^{1/2} - \beta \quad \text{for } \beta \leqslant \tau_\mathrm{H} \leqslant 1/\beta,\ \ \beta \leqslant 1, \tag{10b}$$

$$A^* = \ln(\tau_\mathrm{H}\beta) + 2 - \beta \quad \text{for } 1/\beta \leqslant \tau_\mathrm{H} \leqslant \infty,\ \ \beta \leqslant 1, \tag{10c}$$

$$A^* = \ln \tau_H + 1 \quad \text{for } \tau_H \geqslant 1, \ \beta \geqslant 1, \tag{10d}$$

where $A^* = A/\omega$ is the dimensionless band absorption and τ_H the optical depth at the band head. The transmittance of the band k is calculated from

$$\tau_k = (\tau_H/A)(\mathrm{d}A/\mathrm{d}\tau_H). \tag{11}$$

The width of the band is found by

$$\Delta\nu = A/(1-\tau_k). \tag{12}$$

The transmittance is assumed to be constant within the band limits, which implies a grey band approximation that breaks down at small optical depths. Therefore, Edwards [22] suggested an upper limit of 0.9 on band transmittance. This assumption can cause serious errors if the recurrence relation is employed leading to a strong dependence on the grid resolution (see [21]). Thus, the band limits are defined from the average properties of the whole domain in a preprocessing step. However, the band absorption is still computed from Eq. (10a)–(10d). Therefore, variations in the temperature and composition of the medium are accounted for. The only difference is that instead of calculating first the mean transmissivity from Eq. (11), the bandwidth is prescribed first. The transmittance of the band for a control volume is calculated from

$$\tau_k = 1 - A/\Delta\nu_{\mathrm{fix}} \tag{13}$$

where A is the band absorption for that control volume, and $\Delta\nu_{\mathrm{fix}}$ is the fixed band width calculated in the preprocessing step. It was found that this procedure yields better results than those obtained from Eq. (12) together with the arbitrary upper limit of 0.9 for τ_k. Moreover, the results become less sensitive to the grid resolution. When two or more bands overlap, a new band is created and the transmittance of the overlapping region is equal to the product of the transmittances of the individual bands.

3.2. Integration method

Another method proposed by Cumber et al. [7] is to divide the whole spectrum into several wave number intervals and to calculate the transmittance directly from Eq. (9). The intensity is computed for each interval using a recurrence relation and integrated over the entire spectrum. In this study, either the correlated or the non-correlated formulation is applied, and a mean transmittance of each interval is computed by numerical integration

$$\tau_k = \frac{1}{\Delta\nu}\int_{\Delta\nu} \tau_{\nu,\mathrm{b}}\,\mathrm{d}\nu. \tag{14}$$

Since the model parameters were optimized for the four-region expression, ω was increased by 20% following the recommendations of Edwards [22]. The selection of the band limits does not strongly influence the results [21]. When two or more bands overlap, the total transmittance of the overlapping region is equal to the product of the individual band transmittances.

3.3. Wide band CKM

The EWBM described above yields transmittances whereas for Eq. (1) the absorption coefficient is needed. In the wide band CKM, the wave number spectrum is reordered to yield monotonic decreasing functions of the absorption coefficient around the band centres. The absorption coefficient varies smoothly within each reordered wave number interval so that a discretized set of absorption coefficients is introduced that can easily be applied to Eq. (7). Denison and Fiveland [15] found a simple correlation for the dimensionless reordered wave number ξ^* by a fit to the four-region expression (Eqs. (10a)–(10d))

$$\xi^*(\kappa^*) = \sum_i C_{i,1}E_1(p_i\kappa^*) + C_{1,2}\frac{\mathrm{e}^{-p_1\kappa^*}}{p_1}, \tag{15}$$

where E_1 is the first-order exponential integral function and κ^* is the dimensionless absorption coefficient. The poles p_i and coefficients $C_{i,k}$ are listed in [15]. The reordered wave numbers for band k are given by

$$\xi_k(\kappa_j) = \omega_k\xi^*(\kappa^*) = \omega_k\xi^*\left(\frac{\kappa_j}{p\alpha_k/\omega_k}\right). \tag{16}$$

The weights a_j in Eq. (7) are calculated as blackbody fractions ΔF that correspond to the reordered wave number intervals where the absorption coefficient lies between $\kappa_{j-1/2}$ and $\kappa_{j+1/2}$

$$\begin{aligned} a_j = \sum_k \big\{ & F[\eta_{0,k} - \xi_k(\kappa_{j+1/2})/2, T] \\ & - F[\eta_{0,k} - \xi_k(\kappa_{j-1/2})/2, T] + F[\eta_{0,k} + \xi_k(\kappa_{j-1/2})/2, T] \\ & - F[\eta_{0,k} + \xi_k(\kappa_{j+1/2})/2, T]\big\}. \end{aligned} \tag{17}$$

This equation is valid for a symmetric band centred at wave number $\eta_{0,k}$. Similar expressions may be written for bands with upper or lower limit heads. In this study, 20 grey gases with logarithmically spaced absorption coefficients are used. In the case of non-homogeneous media, the reordered wave numbers are derived from mean temperature and concentrations over the whole domain, whereas the blackbody fractions are computed from the local temperature. The local absorption coefficient is multiplied by the ratio of the local partial pressure of the absorbing gases to the partial pressure averaged over the whole domain. When two or more bands overlap, the individual absorption coefficients are added, and the corresponding blackbody fraction of the overlapping region is contributed to the grey gas j where the sum of absorption coefficients lies between $\kappa_{j-1/2}$ and $\kappa_{j+1/2}$.

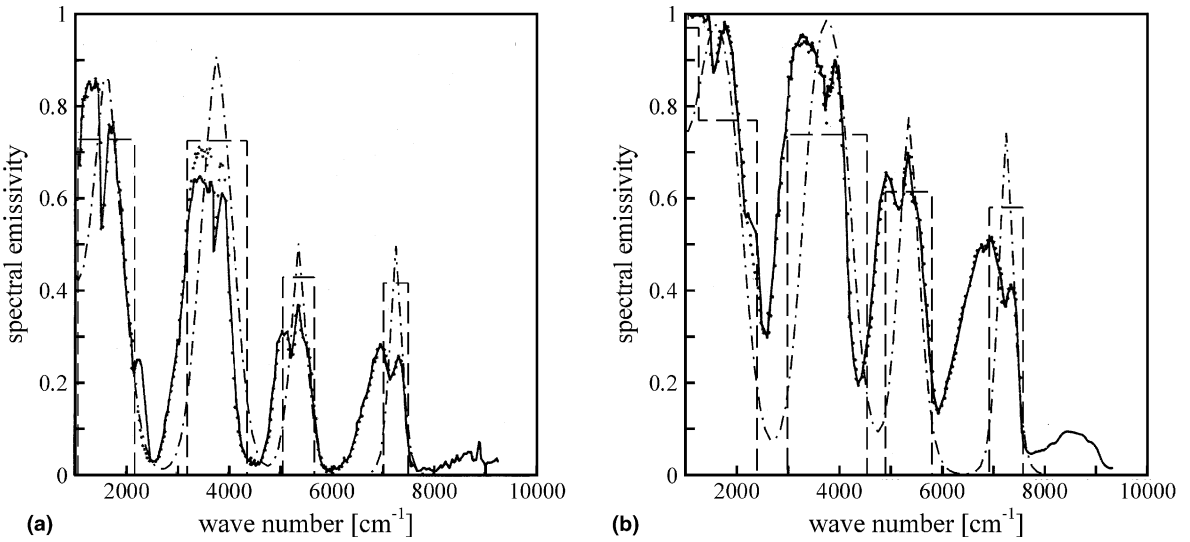

Fig. 3. Experimental (solid line) and computed H_2O spectra with NBM (symbols, taken from [2]), banded method (dashed line) and integration method (dash–dotted lines) at 1500 K (a) and 2500 K (b) with 20 ft path length.

This procedure is also applicable to mixtures of gases under the restriction of a spatially constant ratio of partial pressures of any absorbing gases.

4. Spectral emissivity

In order to investigate the behaviour of the described methods, spectral emissivities computed both from the four-region expression using Eq. (11) and from the spectral transmittance (integration method) using Eq. (9) are compared to experimental and narrow band (NBM) data of Ludwig et al. [2]. Two spectra of water vapour at atmospheric pressure for a path length of 20 ft (6.096 m) at 1500 and 2500 K are shown in Fig. 3. The total emissivities computed from the two different implementations of the EWBM are very close to each other. At 1500 K the EWBM agrees quite well with the experimental data apart from a faulty shape and small shift of the bands to higher wave numbers. This is expected because of the different level of resolution of narrow and wide band models. In fact, both wide and narrow band models use smooth exponential functions to approximate the band shape. However, the width of the bands is greater in wide band models, and therefore it is more difficult for these models to approximate the spectral transmissivity by smooth exponential functions, particularly in the case of band overlapping. Higher differences are observed at 2500 K where the EWBM generally underpredicts the emissivity for all bands. This may be due to the very high temperature and the inherent uncertainty in the spectroscopic data from which the parameters of the wide band model have been obtained. In fact, many spectral lines that are week at low temperatures become important at high temperatures, requiring an extrapolation of experimental data to high temperatures. This means that the data may be quite accurate at low temperatures, but much less accurate at high temperatures.

Two spectra of the 1.87 μm (5350 cm^{-1}) H_2O band at atmospheric pressure for small optical depths are shown in Fig. 4. The partial pressure-path length products are 2.35 and 12.7 cm atm (related to standard density), and the temperatures are 900 and 823 K, respectively. Here

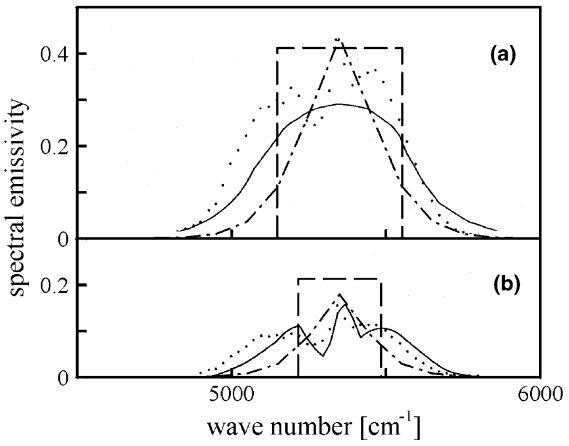

Fig. 4. Experimental (solid line) and computed H_2O spectra at 1.87μ with NBM (symbols, taken from [2]), banded method (dashed line) and integration method (dash–dotted lines) at 900 K with 2.35 cm atm (a) and 832 K with 12.7 cm atm (b).

the EWBM is in fair agreement with the experiments. The integration method can approximately reproduce the shape of the band but slightly underpredicts the total band absorption, which is the area below the curves. These deviations might be due to the fact that the EWBM parameters are optimized for the four-region expression and not for Eq. (9).

5. Radiative transfer in enclosures

Five different approaches of the EWBM described in the previous sections are applied to several test cases. These are the original method using the four-region expression with the correlated (4RM-c) and the non-correlated formulation (4RM-n), the integration method with the correlated (INT-c) and the non-correlated formulation (INT-n), and the wide band CKM that can be solved by the non-correlated formulation. Fixed band limits based on the average properties of the whole domain are used in the 4RM-n.

5.1. One-dimensional enclosure

Radiative transfer between two parallel plates is examined using three different test cases presented by Taine and Soufiani [10]. All configurations are homogeneous with parabolic temperature profiles at atmospheric pressure. Case 1 contains 10% (molar) water vapour and the temperature varies from 2500 K at the wall to 500 K at the centre. Case 2 contains 10% carbon dioxide and the temperature varies from 500 K at the wall to 2500 K at the centre. Both cases have black walls and the path length is varied from 0.1 to 10 m. In case 3, the same temperature and H_2O profiles as in the case 1 are prescribed, but the wall emissivity is varied from 0.05 to 1.0 while the path length is kept constant at 0.2 m. The S_8 discrete ordinates quadrature [23] and 20 equally spaced layers are used for angular and spatial discretizations, respectively. The correlated and non-correlated formulations are based on Eqs. (4) and (5), respectively. One hundred equally spaced wave number intervals are defined for the integration method. In Fig. 5, the

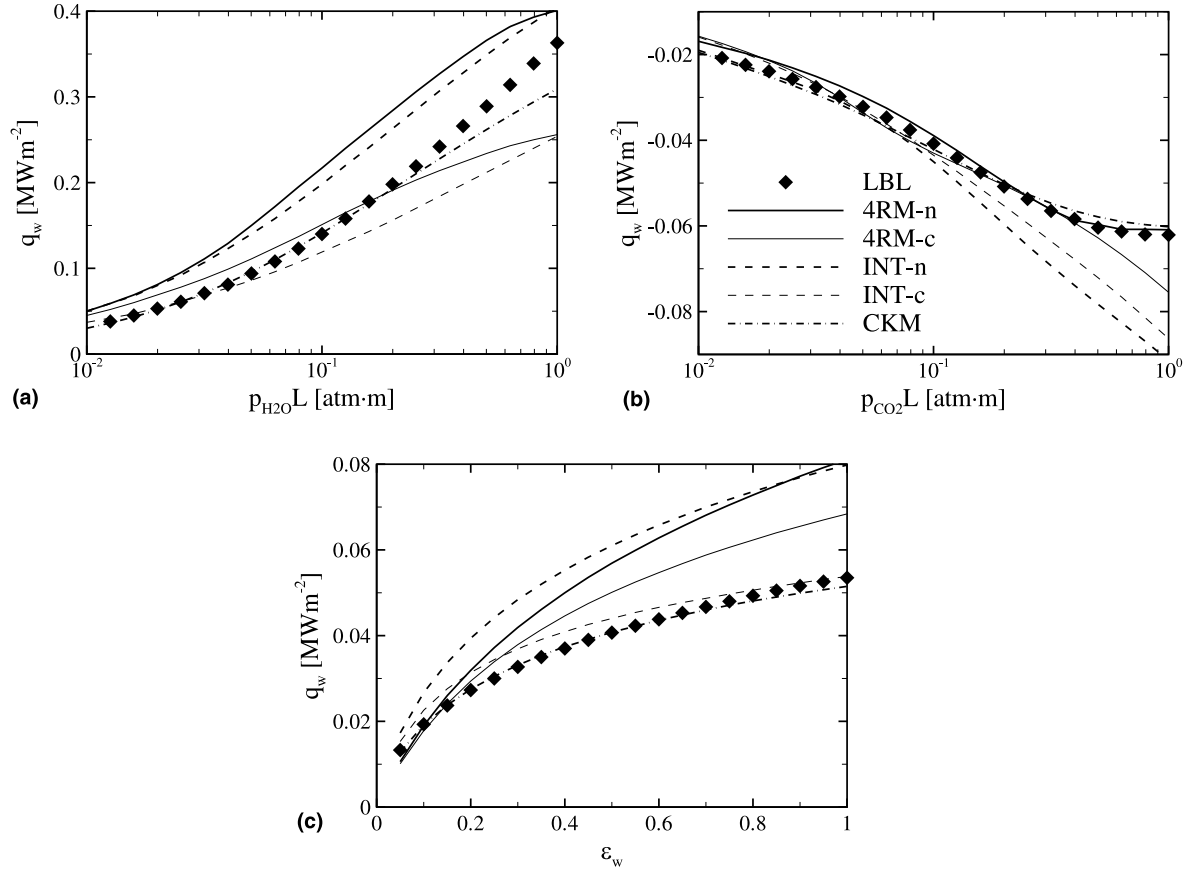

Fig. 5. Computed net wall heat fluxes for one-dimensional test cases. (a) Case 1 – H_2O, black walls. (b) Case 2 – CO_2, black walls. (c) Case 3 – H_2O, grey walls.

computed net wall heat fluxes for these test cases are compared with LBL results of Taine and Soufiani [10] that serve as a reference.

In case 1, the non-correlated methods strongly overpredict the flux by 10–60%, which highlights the shortcomings of the non-correlated formulation. The INT-c is quite accurate for short path lengths, but underpredicts the fluxes by up to 30% for longer path lengths. The 4RM-c overpredicts the fluxes by up to 40% for short path lengths, which might be caused by the upper limit for transmittance, and gets close to the results of the INT-c for long path lengths. The CKM generally yields quite accurate results, but underpredicts the fluxes by up to 14% at very long path lengths. The deviations at long path lengths may be caused by the use of a different spectroscopic data base corresponding to the observations in Fig. 3.

In case 2, the INT-c, 4RM-c and 4RM-n underpredict the flux onto the wall by around 15% for short path lengths, while the integration methods overpredict the flux onto the wall by up to 47% for long path lengths. Strong deviations of the INT-c, due to the fact that the EWBM parameters were optimized for the four-region expression and cannot be adjusted by a constant factor, have already been observed in similar test cases [21]. The block calculation for overlapping bands in the 4RM-c might be the reason for errors of about 21% at long path lengths. The good behaviour of the 4RM-n for long path lengths is surprising. The use of the absorption coefficient as the basic property leads to very good results for the CKM, the error never exceeds 6%.

In case 3, all methods can reproduce the qualitative behaviour of the LBL for varying wall emissivities. The 4RM-c predicts a too strong influence of the wall emissivity on the incident heat flux, and the error of the INT-c increases up to 17% for small wall emissivities. But the large reduction of computational effort, compared to higher order closures, without a serious loss of accuracy justifies the zeroth closure approximation of the correlated methods for grey walls. When the recurrence relation is used, the boundary condition for grey walls do not require any approximation, leading to fair results for small wall emissivities for the non-correlated methods and to very good agreement with LBL results for the CKM.

5.2. Two-dimensional enclosure

Very few radiative transfer calculations in multi-dimensional enclosures with non-grey media have appeared in the literature. Recently, Goutiere et al. [24] presented a comparison of several non-grey gas radiation models for five two-dimensional problems. Three of them are taken here as a basis for comparison of the different wide band model implementations. The geometry used for all test cases is rectangular (1×0.5 m^2), and its walls are black and kept at 0 K. In case 1, the medium is isothermal at 1000 K and homogeneous with 20% (molar) H_2O, while in case 2, the medium is non-isothermal with a non-homogeneous CO_2 profile. In case 3, the medium is non-isothermal and homogeneous with 10% CO_2 and 20% H_2O resembling a gas flame in a furnace. A detailed description of the temperature and concentration profiles can be found in [24]. A uniform grid with 61×31 cells is used for cases 1 and 2, while for case 3, a uniform grid with 81×41 cells is employed. The T_7 quadrature [25] is applied to minimize ray effects. The spatial and angular discretization is identical to that used in [24] allowing a comparison between the present results and those reported there. The correlated and non-correlated formulations are solved using the RTM and DOM, respectively. The wave number intervals for the integration method are defined by the band limits of the four-region expression. The computed wall heat fluxes onto the top wall and the radiative source terms along the horizontal centreline are compared with the narrow band results (NBM) of Goutiere et al. [24] that have been calculated using the RTM and are taken here as a reference solution. Based on this reference solution, the relative errors of the applied methods are listed in Table 1. In the following, a quantitative analysis of the discrepancies is performed and then discussed.

In case 1 (see Fig. 6), the wall heat fluxes of the 4RM-c and CKM are in excellent agreement with the NBM, while the source terms show small deviations of around

Table 1
Mean and maximum (in brackets) relative errors (%) of the computed wall heat flux (Q) and radiative source term (S) from NBM results [24]; computational time for case 3 normalized by the computational time of the fastest method (T)

	Case	4RM-n	4RM-c	INT-n	INT-c	CKM
Q	1	8.4 (10.7)	0.9 (3.9)	15.9 (18.0)	16.2 (17.1)	0.6 (2.9)
	2	3.8 (6.9)	1.2 (2.7)	3.7 (8.0)	5.7 (7.0)	2.0 (2.8)
	3	18.1 (19.8)	5.7 (6.9)	4.5 (5.9)	12.6 (12.9)	1.8 (4.9)
S	1	14.8 (39.7)	5.4 (13.7)	12.4 (46.4)	22.3 (24.3)	7.1 (10.7)
	2	12.9 (43.4)	2.2 (9.1)	7.2 (48.7)	5.5 (14.2)	4.0 (10.5)
	3	23.3 (167.4)	7.9 (40.8)	20.7 (192.5)	10.6 (12.5)	4.3 (22.1)
T	3	1	226.5	2.43	10712.	1.35

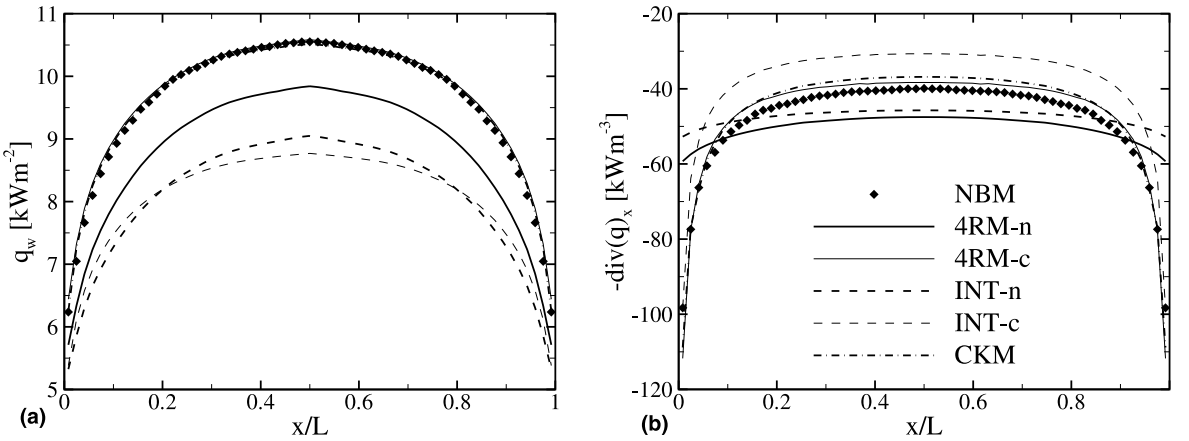

Fig. 6. Incident wall heat flux along the top wall (a) and radiative source term along the centreline (b) for a two-dimensional enclosure with an isothermal, homogeneous medium (20% H_2O).

6%. The INT-c strongly underpredicts both wall heat fluxes and source term by 16% and 22%, respectively. The non-correlated methods do not satisfactorily reproduce the wall heat flux and radiative source term distribution. In case 2 (see Fig. 7), the results of the 4RM-c and CKM are generally very good (the curves of the wall heat fluxes are mostly hidden by the symbols), while the INT-c underpredicts both wall heat fluxes and source terms by around 6%. The non-correlated formulations yield relatively accurate wall heat fluxes, whereas the source terms strongly deviate from the reference values close to the wall. In case 3 (see Fig. 8), the results of the CKM again are very good with a slight overprediction of the source terms by about 4%. The 4RM-c yields source terms of similar accuracy but overpredicts the wall heat fluxes by 6%, whereas the INT-c strongly underpredicts the wall heat fluxes and source terms by 13% and 11%, respectively. The non-correlated methods generally overpredict the wall heat fluxes and show qualitative disagreements of the source term distribution with large errors close to the wall.

From the results presented in Figs. 6–8 and in Table 1, it is concluded that the most accurate results of the described approaches of the EWBM are obtained using the CKM and the 4RM-c. The 4RM-c is the exact formulation of the EWBM in the limit of a homogeneous medium with no band overlapping. The observed discrepancies do not generally exceed 10%, which is well within the margin than can be attributed to differences between wide and narrow band predictions. As in the previous test cases, the relatively large errors of the integration method in some of the test cases are most probably due to the ad hoc increase of ω by 20% relative to the value of ω optimized the

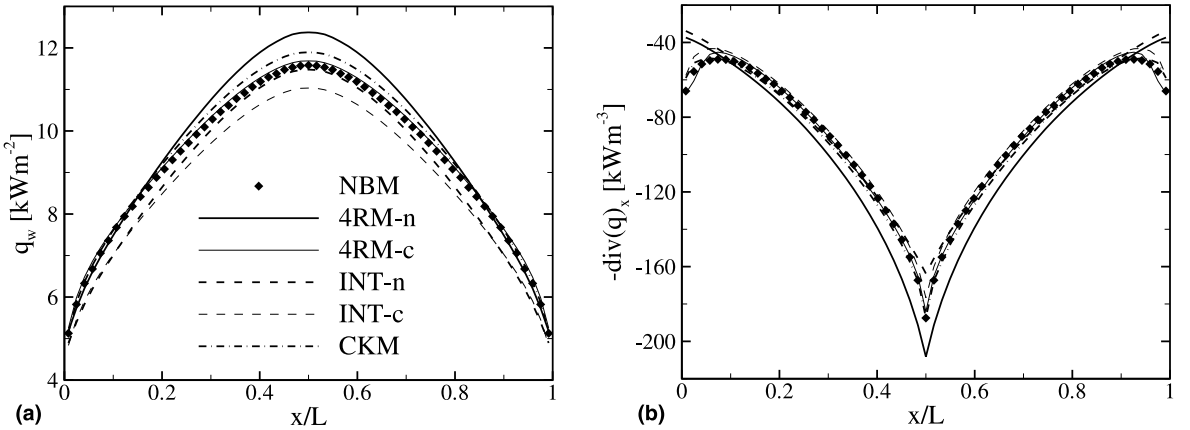

Fig. 7. Incident wall heat flux along the top wall (a) and radiative source term along the centreline (b) for a two-dimensional enclosure with a non-isothermal, non-homogeneous medium (CO_2).

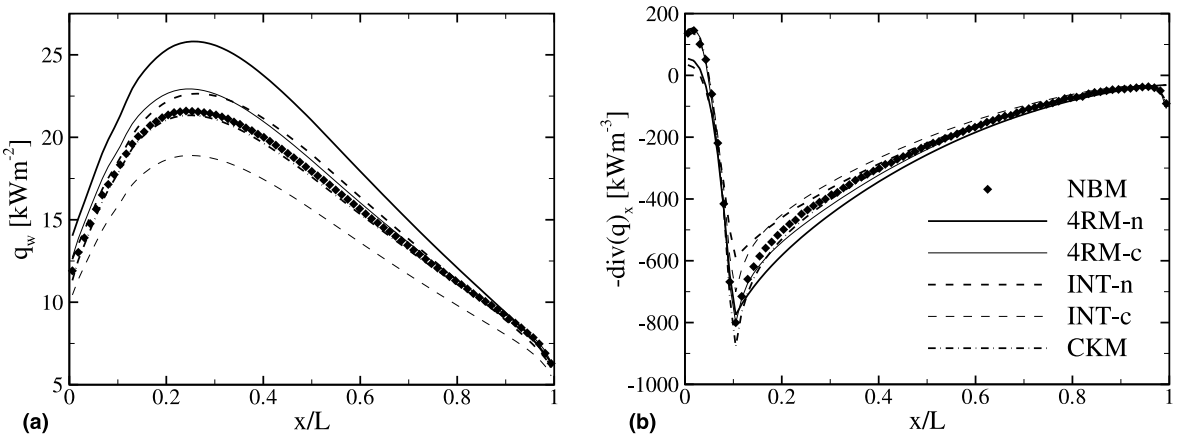

Fig. 8. Incident wall heat flux along the top wall (a) and radiative source term along the centreline (b) for a two-dimensional enclosure with a non-isothermal, homogeneous medium (20% H_2O, 10% CO_2).

four-region expression. The non-correlated formulations (4RM-n and INT-n) generally yield the least accurate predictions, with qualitative inaccurate profiles of the source term distribution in the vicinity of the walls observed in most test cases. This is expected because they neglect the correlation between the radiation intensity and the absorption coefficient, which is not physically realistic.

Finally, the efficiency of the various methods is examined by comparing the computational time needed for one complete run of case 3. In Table 1, values are shown normalized by the computational time of the 4RM-n, which is the fastest method. The computational time for the methods using the DOM are all of the same order of magnitude. The INT-n is about 2.5 times slower than the 4RM-n due to the large effort required to perform the integration over all bands in order to calculate the radiative properties. The computational time for the RTM is two or more orders of magnitude higher than for the DOM. The 4RM-c and the INT-c are about 200 and 4400 times slower than the corresponding non-correlated methods, respectively.

6. Conclusions

Various approaches to the EWBM have been applied to model radiative heat transfer in several one- or two-dimensional enclosures with non-grey media. The formulation of the RTE strongly influences the results and the computational effort. On the one hand the non-correlated formulation can easily be applied to multi-dimensional enclosures, e.g., using the discrete ordinates method, but often leads to large errors and cannot reproduce the shape of the source term distribution. On the other hand the correlated formulation is more accurate, but due to its high computational requirements it is not appropriate for multi-dimensional engineering calculations.

The different implementations of the EWBM also have a strong influence on the accuracy and computational effort. A numerical integration of the spectral transmittance, which is computationally more expensive than the use of the four-region expression, often leads to large errors and is therefore not recommended. The exact application of the four-region expression or the integration method implies the use of a correlated formulation for the solution of the RTE. Therefore, both methods are difficult to apply to multi-dimensional problems, requiring very long computational times. The application of a reordered wave number distribution function allows the use of any radiation solver for both one- and multi-dimensional problems, since the absorption coefficient is the basic radiative property. Combined with the EWBM the wide band CKM has shown to yield very good results without large computational effort. Therefore, it constitutes the best choice for engineering calculations of radiative transfer in multi-dimensional non-grey media.

Acknowledgements

The financial support of the European Commission in the framework of the TMR network, contract no. ERB-FMRX CT98-0224, is gratefully acknowledged.

References

[1] J. Taine, A line-by-line calculation of low resolution radiative properties of CO_2–CO transparent nonisothermal gases mixtures up to 3000 K, J. Quant. Spectrosc. Radiat. Transfer 30 (1983) 371–379.

[2] C.B. Ludwig, W. Malkmus, J.E. Reardon, J.A. Thompson, Handbook of infrared radiation from combustion gases, Technical Report, SP-3080, NASA, Washington, 1973.
[3] D.K. Edwards, A. Balakrishnan, Thermal radiation by combustion gases, Int. J. Heat Mass Transfer 16 (1973) 25–40.
[4] A.T. Modak, Exponential wide band parameters for the pure rotational band of water vapor, J. Quant. Spectrosc. Radiat. Transfer 21 (1979) 131–142.
[5] P. Docherty, M. Fairweather, Predictions of radiative transfer from nonhomogeneous combustion products using the discrete transfer method, Combust. Flame 71 (1988) 79–87.
[6] W. Komornicki, J. Tomeczek, Modification of wide-band gas radiation model for flame calculation, Int. J. Heat Mass Transfer 35 (1992) 1667–1672.
[7] P.S. Cumber, M. Fairweather, H.S. Ledin, Application of wide band radiation models to non-homogeneous combustion systems, Int. J. Heat Mass Transfer 41 (11) (1998) 1573–1584.
[8] A. Arking, K. Grossman, The influence of line shape and band structure on temperatures in planetary atmospheres, J. Atmos. Sci. 9 (5) (1972) 937–949.
[9] G.A. Domoto, Frequency integration for radiative transfer problems involving homogeneous non-gray gases: the inverse transmission function, J. Quant. Spectrosc. Radiat. Transfer 14 (1974) 935–942.
[10] J. Taine, A. Soufiani, From spectroscopic data to approximate models, Adv. Heat Transfer 33 (1999) 295–414.
[11] P.Y.C. Lee, K.G.T. Hollands, G.D. Raithby, Reordering the absorption coefficient within the wide band for predicting gaseous radiant exchange, J. Heat Transfer 118 (1996) 394–400.
[12] G. Parthasarathy, J.C. Chai, S.V. Patankar, A simple approach to non-gray gas modeling, Numer. Heat Transfer B 29 (1996) 113–123.
[13] O. Marin, R.O. Buckius, A simplified wide band model of the cumulative distribution function for water vapor, Int. J. Heat Mass Transfer 41 (1998) 2877–2892.
[14] O. Marin, R.O. Buckius, A simplified wide band model of the cumulative distribution function for carbon dioxide, Int. J. Heat Mass Transfer 41 (1998) 3881–3897.
[15] M.K. Denison, W.A. Fiveland, A correlation for the reordered wave number of the wide band absorptance of radiating gases, J. Heat Transfer 119 (1997) 853–856.
[16] B.G. Carlson, K.D. Lathrop, Transport theory – the method of discrete ordinates, in: Computing Methods in Reactor Physics, Gordon and Breach, New York, 1968.
[17] W.A. Fiveland, Discrete-ordinates solutions of the radiative transport equation for rectangular enclosures, J. Heat Transfer 106 (1984) 699–706.
[18] T.K. Kim, J.A. Menart, H.S. Lee, Nongray radiative gas analyses using the S–N discrete ordinates method, J. Heat Transfer 113 (1991) 946–952.
[19] J.A. Menart, H.S. Lee, T.K. Kim, Discrete ordinates solutions of nongray radiative transfer with diffusely reflecting walls, J. Heat Transfer 115 (1993) 184–193.
[20] L. Zhang, A. Soufiani, J. Taine, Spectral correlated and non-correlated radiative transfer in a finite axisymmetric system containing an absorbing and emitting real gas-particle mixture, Int. J. Heat Mass Transfer 31 (11) (1988) 2261–2272.
[21] P.J. Coelho, J. Ströhle, Different approaches of the exponential wide band model to radiative heat transfer in non-homogeneous media, in: Second International Conference on Computational Heat and Mass Transfer, Rio de Janeiro, Brazil, 2001.
[22] D.K. Edwards, Molecular gas band radiation, Adv. Heat Transfer 12 (1976) 115–193.
[23] M.F. Modest, Radiative Heat Transfer, McGraw-Hill, New York, 1993.
[24] V. Goutiere, F. Liu, A. Charette, An assessment of real-gas modelling in 2D enclosures, J. Quant. Spectrosc. Radiat. Transfer 64 (2000) 299–326.
[25] C.P. Thurgood, A. Pollard, H.A. Becker, The T_N quadrature set for the discrete ordinates method, J. Heat Transfer 117 (1995) 1068–1070.